JOC The Journal of Organic Chemistry

Article

pubs.acs.org/joc

Photoluminescence, Redox Properties, and Electrogenerated Chemiluminescence of Twisted 9,9′-Bianthryls

Palani Natarajan* and Michael Schmittel*

Center of Micro- and Nanochemistry and Engineering, Department of Chemistry and Biology, Organische Chemie I, Universität Siegen, Adolf-Reichwein-Straße 2, D-57068 Siegen, Germany

Supporting Information

ABSTRACT: To study the dual emission (from locally excited and charge transfer states) of sterically crowded 9,9′-bianthryl (**BAHO**) and its 10,10′-disubstituted derivatives, namely, 10,10′-dibromo-9,9′-bianthryl (**BABR**), 10,10′-bis(*p*-tolylethynyl)-9,9′-bianthryl (**BAET**), and 10,10′-bis(*N*,*N*-diphenyl-4-anilino)-9,9′-bianthryl (**BATA**) in detail, we probed their photophysical, redox, and electrogenerated chemiluminescence (ECL) responses. Dual emission for all of the molecules was noticed in PL, whereas in ECL only charge transfer emission was observed over a variety of experimental conditions. The PL in nonpolar solvents is significantly influenced by added supporting electrolyte, yielding exclusively charge transfer emission as in ECL. The stability of ECL proved to depend largely on the nature of the substituent, with triarylamine and bromo groups imparting constant ECL intensity over more than 60 cycles.

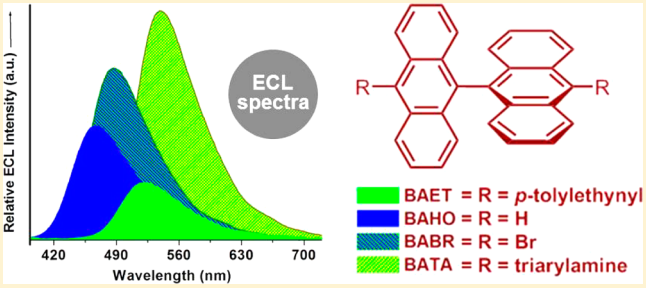

INTRODUCTION

Among organic compounds that are active in electrogenerated chemiluminescence (ECL, also called electrochemiluminescence),[1] bulky and rigid as well as awkwardly shaped molecules often provide constant ECL intensity over several potential scans with high quantum yield (ϕ_{ECL}), independent of the use of annihilation or coreactant ECL.[2] Electrochemically produced radical ions of awkwardly shaped structures are often spared from unwanted self-combinations toward dimers or polymers as well as external attack of water/oxygen as a result of steric hindrance or bulky substituents in the scaffold.[3] Chart 1 shows the structures of awkwardly shaped molecules whose redox and ECL behaviors have been reported recently.[4] Notably, all of these molecules exhibit moderate to good ECL signals with comparable quantum efficiencies. For example, the triarylamine-decorated spirobifluorenes[4h] 2,7-bis(4-*N*,*N*-diphenylaminophenyl)-9,9′-spirobifluorene and 2,2′,7,7′-tetrakis(4-*N*,*N*-diphenylaminophenyl)-9,9′-spirobifluorene (Chart 1) showed reversible oxidation and reduction during electrolysis and furnished a static greenish-blue ECL with a constant intensity over several potential scans. The rigid spiro linkage prevents excimer formation (responsible for nonradiative decay of excited-state photons) between the 2,7-bis(4-*N*,*N*-diphenylaminophenyl)-fluorene units even at high concentration.[4h] As a result, ϕ_{ECL} was found to be about 3 times higher than that of 9,10-diphenylanthracene (DPA),[1] a familiar ECL standard. To date, only a couple of awkwardly shaped organic molecules have been reported in ECL research because of arduous accessibility.[1,2,4] Therefore, the fabrication of related bulky and rigid organic materials from readily available precursors has been actively pursued in both academic and industrial research.[5]

9,9′-Bianthryl[6] and its derivatives[6c,e] (here called "bianthryls") are bulky and conformationally restricted structures that are easily accessible by zinc-mediated reductive coupling of the corresponding 9-anthrones. Because of the intramolecular H−H repulsion between hydrogen atoms at the 1,1′- and 8,8′-positions, the two anthracene chromophores are oriented perpendicular to each other with dihedral angles of 82°−86° depending on the substituents.[6] As a consequence, the HOMO−LUMO energy gaps and photophysics of bianthryls roughly resemble those of arylanthracenes.[6c,d,7] Nevertheless, their photochemical and electrochemical properties are quite useful because bianthryls undergo neither photochemical oxidation[8] nor electrochemical decomposition,[9] quite in contrast to the situation in arylanthracenes.[10] Accordingly, bianthryls have been extensively utilized in non-photodegradable electroconducting films,[9] photovoltaic cells,[11] electrochromic materials,[11b] and so on.[6,11c]

Over the years, we have rationally designed and explored ECL probes based on ruthenium(II) and iridium(III) complexes for applications such as lab-on-molecules[12] as well as on rigid anthracenes[13] that are inert toward singlet oxygen and water during photo- and electrochemical initiation. In continuation, we report herein the synthesis of the 9,9′-bianthryls **BAHO**, **BABR**, **BAET**, and **BATA** (Chart 2) and their photophysical,[14,15] redox, and ECL behaviors in nonaqueous solvents. They were expected to exhibit (i) high PL quantum yield, (ii) solvatochromic and environment-dependent fluorescence, and (iii) good solubility both in nonpolar and polar solvents. The use of triarylamine, *p*-tolylethynyl, and bromo substituents in **BATA**, **BAET**, and

Received: August 14, 2013
Published: September 12, 2013

   dx.doi.org/10.1021/jo401785c | *J. Org. Chem.* 2013, 78, 10383−10394

Chart 1. Structure of Awkwardly Shaped Molecules Whose Redox and ECL Behaviors Have Been Reported Previously[4]

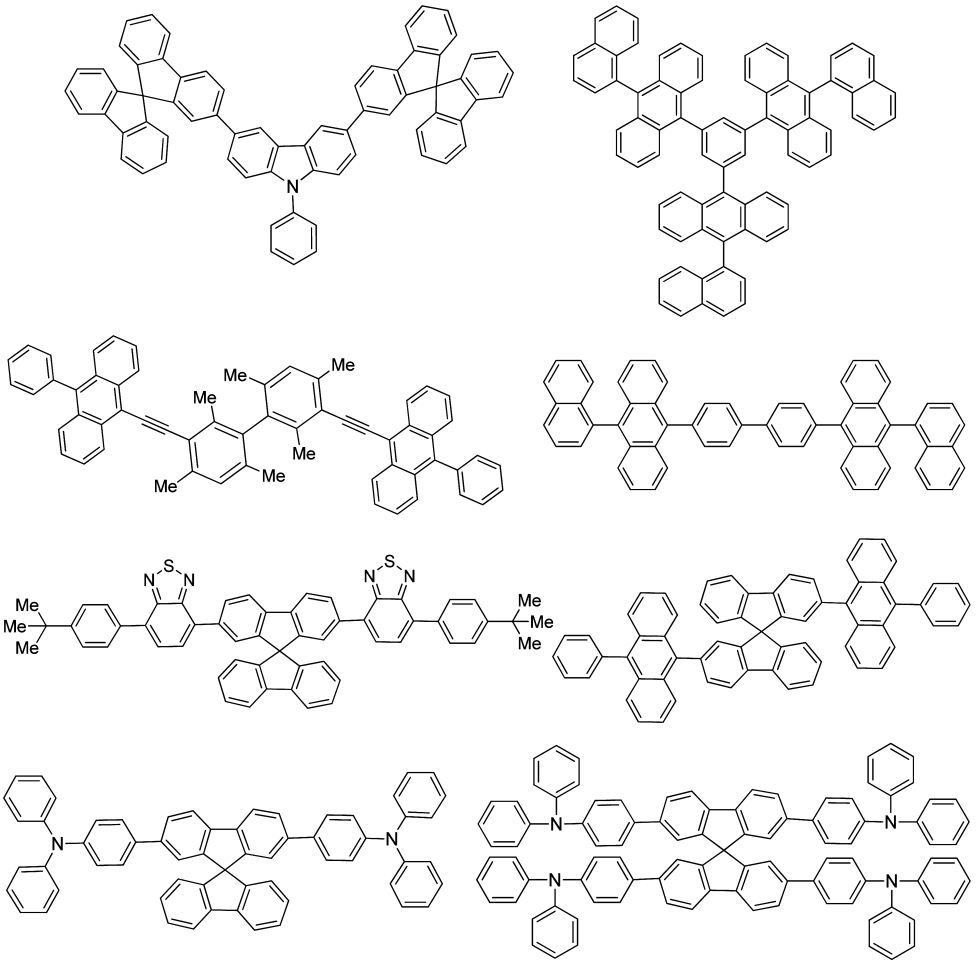

Chart 2. Molecular Structures of the Bianthryls BAHO, BABR, BAET, and BATA

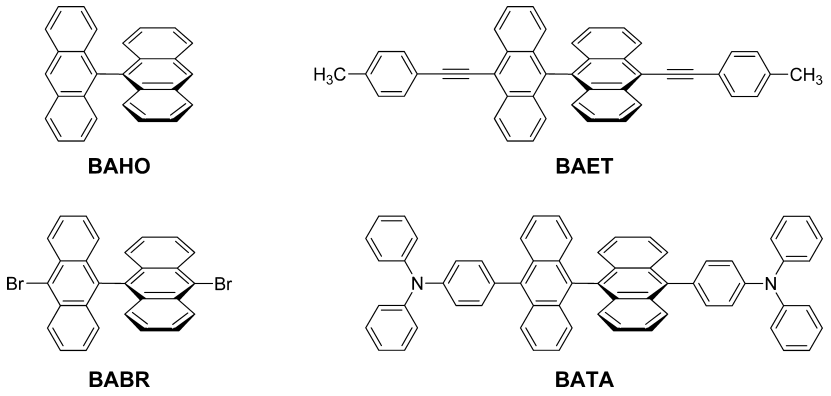

BABR, respectively, was supposed to give the bianthryl unit easy oxidizability or reducibility, high photo- and thermal stability, and/or wide color tunability, depending on their electronic character.[5f,12]

RESULTS AND DISCUSSION

Synthesis and Characterization. The bianthryls **BAHO**, **BABR**, **BAET**, and **BATA** (Chart 2) were readily synthesized by following the routes given in Scheme 1. Zn/$ZnCl_2$-mediated reductive dimerization of 9-anthrone yielded 10,10′-tetrahydro-9,9′-dihydroxybianthryl, which was subjected to azeotropic dehydration in toluene to provide 9,9′-bianthryl (**BAHO**) in quantitative yield.[6b] Electrophilic bromination of **BAHO** in CCl_4 with Br_2 furnished 10,10′-dibromo-9,9′-bianthryl (**BABR**) in 86% yield.[16] The latter was reacted in a Pd-mediated Suzuki coupling with 4-*N*,*N*-diphenylaminophenylboronic acid and in a Sonogashira cross-coupling protocol with *p*-tolylethynyl, affording **BATA** and **BAET**, respectively (Scheme 1). All of the compounds were purified by silica-gel column chromatography and characterized by elemental analysis as well as IR and ^1H, ^{13}C, and COSY NMR spectroscopy [see the Supporting Information (SI)].

dx.doi.org/10.1021/jo401785c | J. Org. Chem. 2013, 78, 10383−10394

Scheme 1. Synthetic Routes to the Bianthryls BAHO, BABR, BAET, and BATA

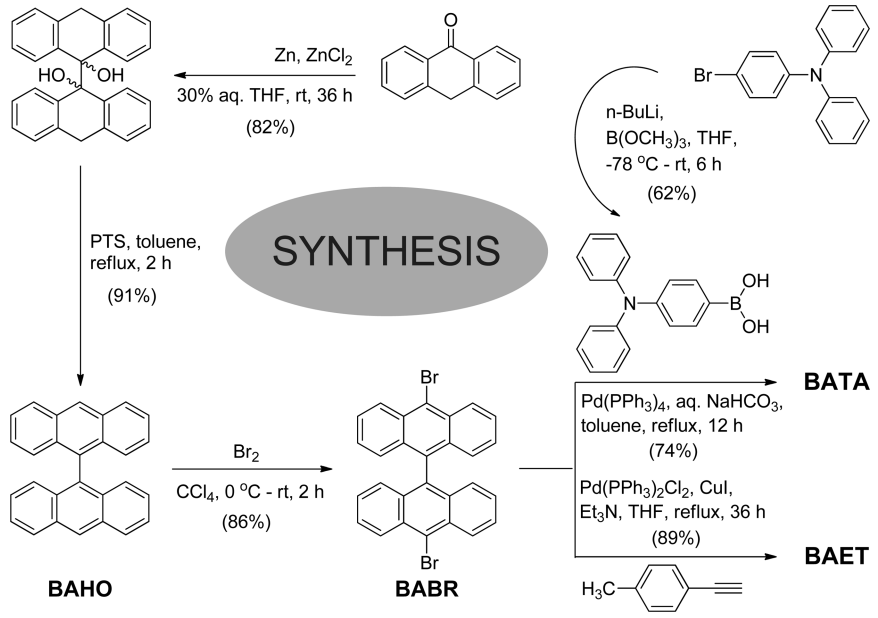

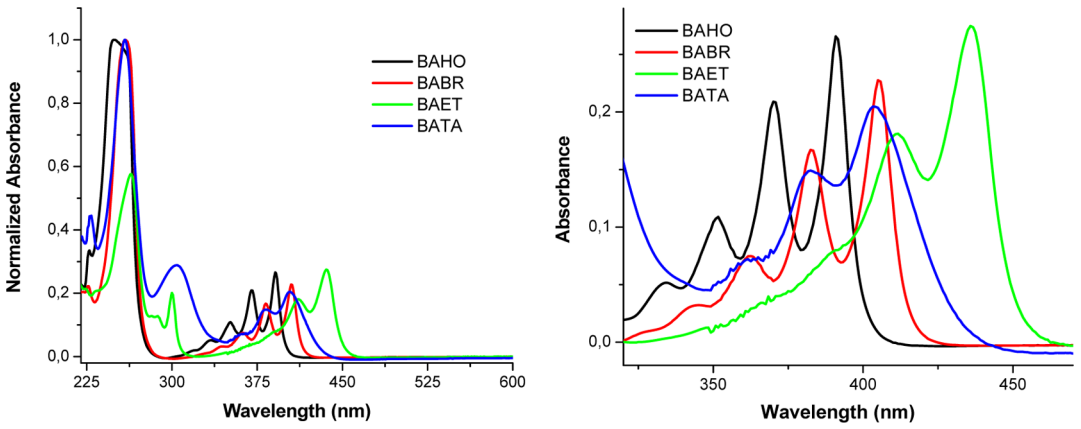

Figure 1. UV−vis absorption spectra of **BAHO**, **BABR**, **BAET**, and **BATA** in DCM. On the right side, the expanded visible region is shown.

As 9,9′-bianthryls lack the ability to undergo $\pi-\pi$ stacking,[6] they show good solubility both in nonpolar and polar solvents of different dielectric constants (ϵ). As such, **BAHO**, **BABR**, **BAET**, and **BATA** (Chart 1) exhibit decent solubility (7×10^{-4} M) even in highly polar acetonitrile (polarity index $P' = 6.2$ and $\epsilon = 37.5$), allowing us to explore measurements in more than one solvent.

Photophysical Properties. It is well-known that the energy levels of symmetrical biaryls can be modulated by the medium.[14,17] Thus, absorption and emission spectra were recorded in four solvents having different attributes. The UV−vis absorption spectra of **BAHO**, **BABR**, **BAET**, and **BATA** in dichloromethane (DCM) are shown in Figure 1, and the profiles in other solvents [i.e., methylcyclohexane (MCH), tetrahydrofuran (THF), and acetonitrile (ACN)] are presented in the SI. Table 1 contains the wavelengths of absorption (λ_{abs}) and molar extinction coefficients (ε) for the entire series of solvents. All of the bianthryls in Chart 2 exhibit a short-wavelength β-band between 220 and 290 nm that is characteristic for any anthracenyl derivative[13] and a structured long-wavelength $\pi-\pi^*$ transition in the visible region at 350−465 nm for which λ_{max}^{abs} varies with the nature of the substituents. The extensive π-conjugation with the *p*-tolylethynyl groups in **BAET** raises the HOMO energy and lowers the LUMO energy, furnishing the most red-shifted (by ca. 48 nm) λ_{max}^{abs} in the series (Table 1). Likewise, the electron-deficient bromo groups in **BABR** and electron-rich triarylamine substituents in **BATA** affect both the LUMO and HOMO levels of the bianthryl residue as well but provide a moderate red shift (ca. 15 nm) relative to **BAHO**. Thus, the energy levels of bianthryls can be altered readily by functionalization.

In contrast to the above-mentioned substituent effects, the solvent properties (polarity and ϵ) do not influence the energies of the bianthryls at all (Chart 2). For example, the values of λ_{max}^{abs} for **BAHO** in MCH, THF, DCM, and ACN are 390, 391, 391, and 388 nm, respectively, suggesting that the ground states of all these bianthryls are rather nonpolar in nature.[14,17] In addition, the medium does not induce any changes in the conformation or the dihedral angle between the conjoined anthracenyl units, because the profile shapes (Figure 1) and λ_{abs} values (Table 1) for **BAHO**, **BABR**, **BAET**, and **BATA** in all solvents are roughly similar to those of the corresponding half-components [i.e., λ_{abs} = 254, 329, 344, 363, and 382 nm for anthracene; λ_{abs} = 258, 339, 357, 375, and 395 nm for 9-bromoanthracene; λ_{abs} = 266, 304, 386, 403, and 426 nm for 9-(*p*-tolylethynyl)anthracene; and

dx.doi.org/10.1021/jo401785c | J. Org. Chem. 2013, 78, 10383−10394

Table 1. Photophysical Data for the Bianthryls Shown in Chart 2

compound	solvent (ϵ)[a]	λ_{abs} (nm)[b]	ε (10^4 M^{-1} cm^{-1})[c]	λ_{max}^{PL} (nm)[d]	ϕ_{PL}[e]	$\Delta\lambda_{Stokes}$ (nm)[f]
BAHO	MCH (1.89)	252, 333, 352, 370, **390**	2.1	411	0.52	21
	THF (7.52)	257, 333, 350, 370, **391**	2.3	423	0.51	32
	DCM (9.08)	253, 333, 352, 371, **391**	2.4	446	0.51	55
	ACN (37.5)	251, 331, 349, 368, **388**	2.8	462	0.18	74
BABR	MCH (1.89)	259, 343, 362, 383, **405**	1.7	412	0.11	7
	THF (7.52)	260, 342, 362, 383, **406**	1.8	435	0.10	29
	DCM (9.08)	259, 344, 362, 382, **406**	1.7	457	0.09	51
	ACN (37.5)	258, 342, 360, 380, **402**	1.9	483	0.04	81
BAET	MCH (1.89)	267, 303, 392 (sh), 415, **440**	7.2	458	0.71	18
	THF (7.52)	268, 303, 389 (sh), 414, **440**	7.6	475	0.68	35
	DCM (9.08)	265, 301, 391 (sh), 411, **437**	7.8	490	0.68	53
	ACN (37.5)	264, 301, 391 (sh), 411, **436**	8.2	519	0.24	83
BATA	MCH (1.89)	259, 304, 359, 382, **404**	2.6	434	0.84	30
	THF (7.52)	255, 301, 357, 378, **401**	2.6	476	0.46	75
	DCM (9.08)	259, 303, 360, 383, **405**	2.7	496	0.44	91
	ACN (37.5)	255, 301, 359, 381, **401**	2.9	528	0.26	127

[a]Doubly distilled solvents were used. Abbreviations: MCH, methylcyclohexane; THF, tetrahydrofuran; DCM, dichloromethane; ACN, acetonitrile. [b]Absorption spectra were measured for 1×10^{-5} M solutions. The lowest-energy band is highlighted in bold. sh, shoulder. [c]The molar extinction coefficient (ε) was determined for ca. 1×10^{-5} M solution at the lowest-energy absorption. [d]Recorded using $1-10 \times 10^{-6}$ M solutions with an excitation wavelength of 360 ± 5 nm. [e]Measured with reference to 9,10-diphenylanthracene with $\phi_{PL} = 0.9 \pm 0.02$ in cyclohexane. [f]Calculated energy difference between the lowest energy absorption band and λ_{max}^{PL}.

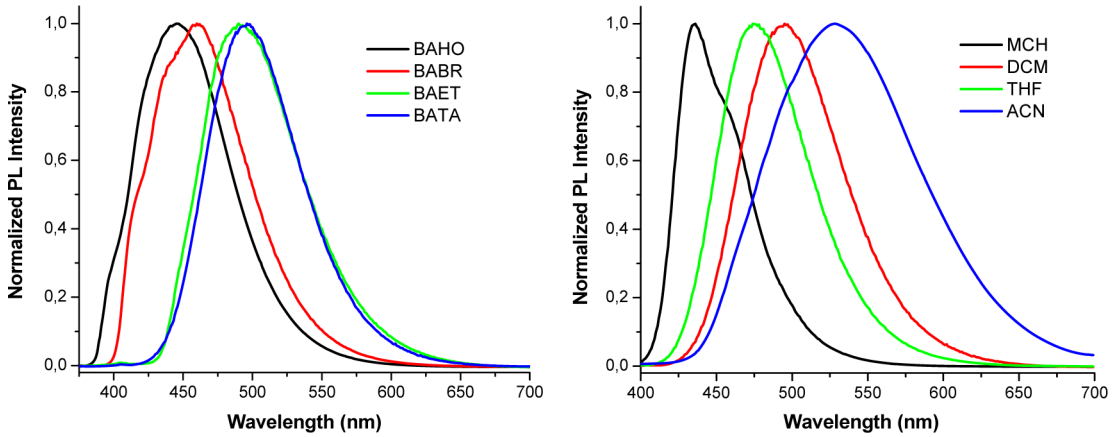

Figure 2. (left) Typical PL spectra of **BAHO**, **BABR**, **BAET**, and **BATA** in DCM. (right) PL spectra showing the positive solvatochromic behavior of **BATA** in MCH, DCM, THF, and ACN as seen from the wavelength shift (λ_{exc} = 360 ± 5 nm).

λ_{abs} = 263, 305, 361, 379, and 399 nm for 9-(*N*,*N*-diphenyl-4-anilino)anthracene]. Thus, it is reasonable to assume that the two aromatic halves are perpendicular to each other in solution. This interpretation is in line with previously determined dihedral angles of the two anthracenyl planes of 9,9′-bianthryl and its 10,10′-functionalized derivatives in solution[18] (ca. 80.5−88.7°) as well as in the solid state[6] (ca. 81.5−85.9°). The experimental ε values of the bianthryls in Chart 2 at the absorption maxima were found to be almost twice those of analogous monoanthracenes (Table 1).

Figure 2 shows typical PL spectra of **BAHO**, **BABR**, **BAET**, and **BATA** in DCM at room temperature, which display emission wavelength maxima (λ_{max}^{PL}) in the range of 445−495 nm, corresponding to indigo to green light. Clearly, λ_{max}^{PL} is influenced by the electronic nature of the 10,10′-substituents. In DCM the bromo substituents red-shift λ_{max}^{PL} by 10 nm relative to the parent **BAHO**, whereas *p*-tolylethynyl and triphenylamine functionalities red-shift λ_{max}^{PL} by 44 and 50 nm.[19] To examine the effect of the medium on the excited state of the bianthryls in Chart 2, the PL was measured in MCH, THF, and ACN as well (Figure 2 and Table 1; also see the SI). The λ_{max}^{PL}, profile shape, and emission quantum yield of bianthryls are considerably altered depending on the solvent characteristics (vide infra). The λ_{max}^{PL} of **BAHO** is red-shifted by ca. 51 nm from violet (411 nm) to blue (462 nm) with the change from nonpolar MCH to highly polar ACN (positive solvatochromism).[19] Analogous red-shifted emissions are equally seen for all of the 10,10′-disubstituted bianthryls, but the values are much higher, ca. 70, 60, and 95 nm for **BABR**, **BAET**, and **BATA**, respectively, possibly as a result of combined medium and substituent effects.[17] In addition, the profile gradually loses its vibronic structure, thus attaining an unstructured feature in going from less to more polar solvents. The emission of **BATA**, shown in Figure 2, exhibits a structured pattern with λ_{max}^{PL} centered at 434 nm in MCH, whereas in ACN the emission is almost structureless at λ_{max}^{PL} = 528 nm, suggesting solvation effects on the excited state. The changes in the excited-state energy can be depicted in the form of Stokes shifts ($\Delta\lambda$)[20] by comparing them with ground-state energies. The values of $\Delta\lambda$ between the lowest-energy absorption peak and the emission maximum of the bianthryls vary from 7 nm (ca. 419 cm^{-1}) to 127 nm

dx.doi.org/10.1021/jo401785c | J. Org. Chem. 2013, 78, 10383−10394

(ca. 5999 cm^{-1}) (Table 1). The changes in λ_{max}^{PL} and the profile shape against the solvent attributes suggest that the emission may arise from more than one state or species.[19] In order to examine whether excimers are involved upon changing the medium, we recorded excitation and emission spectra of the bianthryls in the concentration range from 10^{-6} to 10^{-4} M. Likewise, emission spectra were recorded at different excitation wavelengths from 275 to 375 nm, and reciprocally, excitation spectra were measured at varying emission wavelengths from 400 to 550 nm (see the SI). In all of these measurements, the shape of the emission profile, λ_{max}^{PL}, and $\Delta\lambda$ remained independent of the concentration. Moreover, the excitation spectra of the bianthryls are autonomous with respect to the emission wavelength as well as solvent attribute, viz., the excitation spectra are roughly superimposable on their absorption spectra in any of the solvents. Only the spectral intensity went up or down depending on the concentration and the value of excitation/emission wavelength used. From these combined observations, we conclude that (i) excimer formation is unlikely[19] and (ii) the emissions of **BAHO**, **BABR**, **BAET**, and **BATA** originate exclusively from a sole excited species that has two energetically dissimilar emitting states stabilized to various extents according to the nature of the medium.[14,17]

Normally, symmetrical biaryls lose their symmetry in the excited state[14,17,21] by an intramolecular charge transfer (ICT) linking the locally excited (LE) state to a charge transfer (CT) state (Scheme 2) with equilibration on the picosecond scale.[22]

Scheme 2. Electronic-State Dynamics of Photoexcited 9,9′-Bianthryl and Its Energy Levels

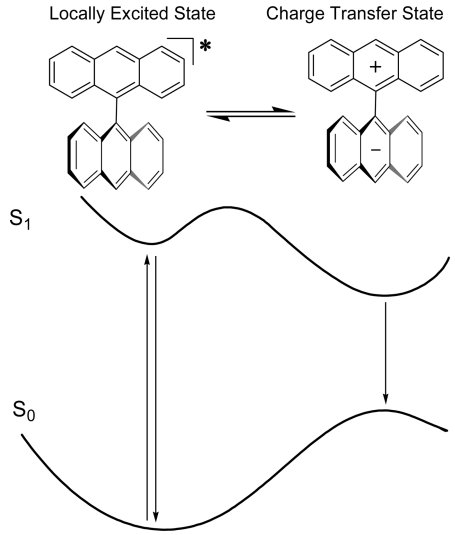

The LE ⇄ CT equilibrium completely shifts toward the CT state in highly polar solvents such as ACN and DMSO.[14,17] In ACN, though, only a broad band due to CT emission was observed (Figure 2 and Table 1). The persistence of structured vibronic bands at the blue edge next to a broad emissive band in MCH, THF, and DCM suggests that here the emission arises from both the LE and CT excited states (Scheme 2). A similar behavior has been noticed for other rigid symmetrical biaryls.[17,23] The maximum solvent-induced red shift from 434 to 528 nm (Stokes shift = 127 nm) as observed in the case of **BATA** is due to the strong electron donation by the triarylamine groups, which are known to promote efficient ICT in the excited state.[24]

The emissions of all of the bianthryls in Chart 2 were quantified by PL quantum yield (ϕ_{PL}) measurements using DPA ($\phi = 0.9 \pm 0.02$ in cyclohexane) as a standard.[25] As expected, the ϕ_{PL} values for all of the bianthryls decrease with increasing polarity and ϵ of the medium because of competing excited-state quenching of the fluorescence by electron transfer.[14,17,21−24] In MCH ($\epsilon = 1.89$), ϕ_{PL} of **BATA** is 0.84, while it is reduced to 0.26 in ACN ($\epsilon = 37.5$), demonstrating that strong ICT occurs in these bianthryls (Table 1).

Electrochemical Data. Cyclic voltammograms (CVs) were recorded to study the redox behavior of the bianthryls (5×10^{-4} M) with 0.1 M tetra-*n*-butylammonium hexafluorophosphate ($TBAPF_6$) as a supporting electrolyte in DCM [scan rate (ν) = 50 mV s^{-1} for oxidation] and in ACN (ν = 100 mV s^{-1} for reduction). The oxidation and reduction peak potentials are reported with reference to ferrocene/ferrocenium (Fc/Fc^+) in Table 2.

Oxidation. Typical CVs are shown in Figure 3, with two defined anodic waves for **BAHO** at +0.85 and +1.12 V vs Fc/Fc^+. The first peak is completely reversible, whereas the second peak is quasi-reversible with an unequal peak current. The peak separation of the first wave is ca. 78 mV, equally observed for the internal standard Fc/Fc^+ under the same experimental conditions, hinting a one-electron transfer reaction.[26] The quasi-reversible behavior of **BAHO** did not improve even at higher scan rates up to 500 mV s^{-1} (see the SI). The peak current of the second wave corresponds to ca. 6 μA, which is double the value of the first wave, suggesting that the second peak involves two sequential one-electron oxidation steps (i.e., formation of $BAHO^{2+}$ and $BAHO^{3+}$ from $BAHO^{+\bullet}$). Such a feature has been reported for several molecular orthogonal systems with two identical electrophores conjoined without ample communication.[27]

BABR and **BAET** undergo two reversible one-electron oxidations with $E_{1/2}^{ox}$ centered at 0.97 and 1.22 V vs Fc/Fc^+ and 0.76 and 1.01 V vs Fc/Fc^+, respectively. Thus, both the *p*-tolylethynyl and bromo substituents stabilize the monocharged (+•) and dicharged (2+) species.[28] The potential ranges nicely agree with the UV−vis findings in that effective π-conjugation between the *p*-tolylethynyl and bianthryl unit elevates the HOMO level of **BAET**, thus shifting the oxidation to lower potentials.[3]

In contrast to the other bianthryls, a 4+ charged ion (Figure 3) was observed for **BATA** upon oxidation even at a scan rate of 50 mV s^{-1}. Because of its good donor quality, the triarylamine unit undergoes oxidation at lower potentials (0.3−0.5 V vs Fc/Fc^+) than the anthracenyl framework.[28] In the voltammogram of **BATA**, the first three fully reversible peaks are assigned to one-electron oxidation events of both triphenylamine units (0.35 and 0.53 V vs Fc/Fc^+) and the bianthryl (0.88 V vs Fc/Fc^+).[9] The fourth oxidation peak (1.10 V vs Fc/Fc^+) representing the formation of $bianthryl^{2+}$ is quasi-reversible (Table 2).

Reduction. While cathodic reduction of the bianthryls in Chart 2 in DCM at scan rates of 50 to 200 mV s^{-1} produces an irreversible reduction peak, in ACN, except for **BABR**, the potential−current curves exhibit reversible waves at a scan rate of 100 mV s^{-1}. **BAHO**, **BAET**, and **BATA** undergo two-electron reduction in a sequential manner, with the first reduction wave being reversible at $E_{1/2}^{red} = -1.32$ V (**BAHO**), −1.03 V (**BATA**), and −0.88 V (**BAET**). A reversible doubly charged anion, $BAET^{2-}$ (at −1.04 V vs Fc/Fc^+), is seen only with *p*-tolylethynyl substituents.[28] In contrast, second reduction signals for **BAHO** and **BATA** are only quasi-reversible (see the SI). As expected, the

dx.doi.org/10.1021/jo401785c | J. Org. Chem. 2013, 78, 10383−10394

Table 2. Electrochemical and ECL Data for the Bianthryls Shown in Chart 2

			ECL λ_{max} (nm)[d]		ϕ_{ECL}[e]	
compound	$E^{ox}_{1/2}$ (V vs Fc/Fc$^+$)[a,b]	$E^{red}_{1/2}$ (V vs Fc/Fc$^+$)[a,c]	DCM	ACN	DCM	ACN
BAHO	+0.85, +1.12*	−1.32, −1.55*	469	472	1.0 ± 0.4	0.7 ± 0.3
BABR	+0.97, +1.22	ND	486	487	1.4 ± 0.1	1.2 ± 0.1
BAET	+0.76, +1.01	−0.88, −1.04	520	522	0.9 ± 0.2	0.8 ± 0.3
BATA	+0.35, +0.53, +0.88, +1.10*	−1.03, −1.39*	538	537	2.5 ± 0.1	2.3 ± 0.1

[a]Potentials of all compounds (5×10^{-4} M) were obtained from cyclic voltammetry and are referenced to Fc/Fc$^+$. Asterisks (*) indicate either quasi-reversible or irreversible waves. [b]In DCM at a scan rate of 50 mV s^{-1}. [c]In ACN at a scan rate of 100 mV s^{-1}. ND, not determinable. [d]ECL measured for samples (5×10^{-4} M) in the presence of 100 mM tri-*n*-propylamine (TPrA) in DCM or ACN. [e]ϕ_{ECL} is the ECL intensity relative to that of DPA, which is taken as unity. Values are averages of at least five independent experiments in DCM or ACN. The ϕ_{ECL} values are 7−11% greater in DCM than in ACN.

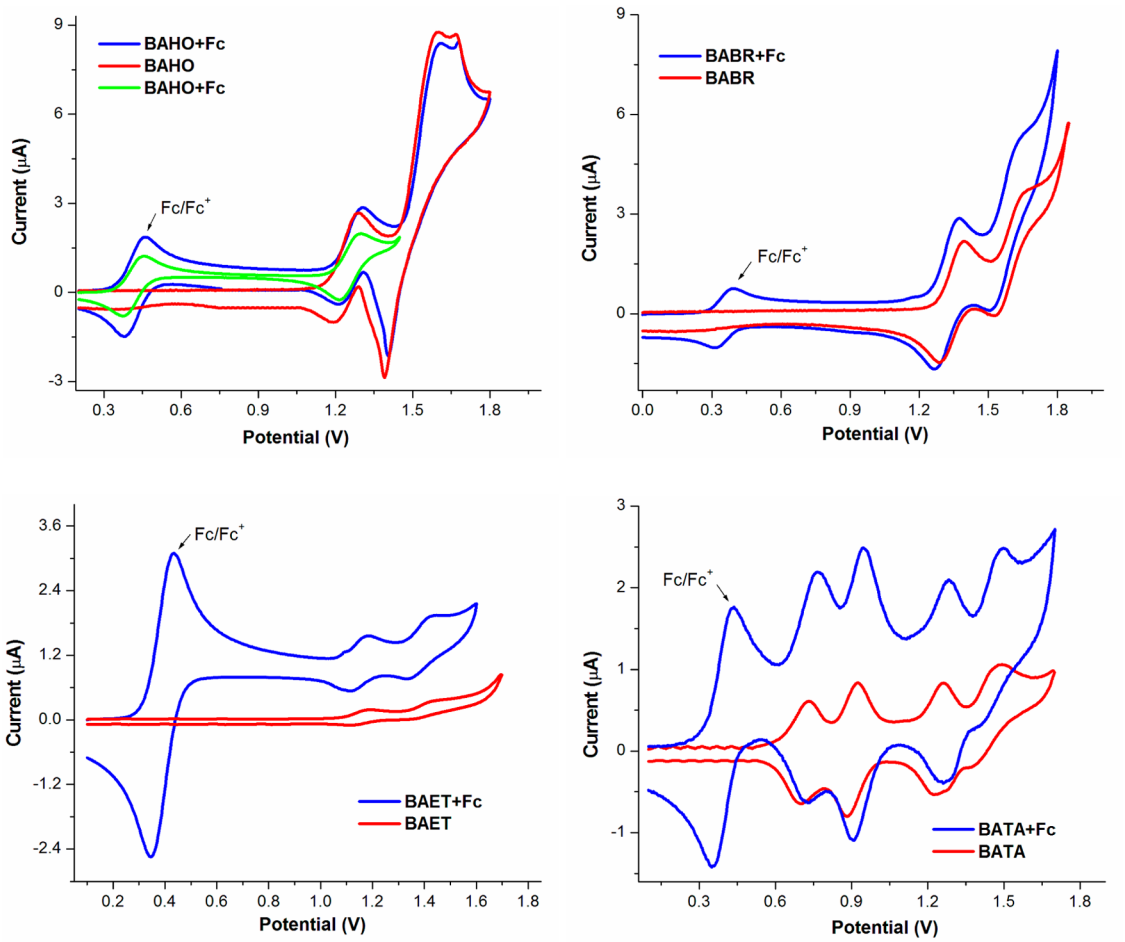

Figure 3. CVs of **BAHO**, **BABR**, **BAET**, and **BATA** (5×10^{-4} M) in DCM at a scan rate of 50 mV s^{-1}. The blue and green profiles of **BAHO** obtained by sweeping the electrode potential from 0 V to 1.8 V and 0 V to 1.4 V, respectively.

strong electron donation of the triarylamine groups of **BATA** destabilizes the anionic species.[3]

An irreversible reduction peak was observed for **BABR** in DCM, ACN, or 30:70 DMF/ACN at different scan rates and is most likely due to electrochemical cleavage of the C−Br bond. Such a process is well-known. For example, 9,10-dichloro- and 9,10-dibromoanthracenes yield mixtures of anthracene and 9,10-dihydroanthracene after electrochemical reduction.[29]

Interestingly, the oxidation and reduction potentials of the bianthryls in Chart 2 are in the same range as $E^{ox}_{1/2}$ and $E^{red}_{1/2}$ of the corresponding half-components measured under the same conditions [i.e., +0.86 and −1.27 V vs Fc/Fc$^+$ for anthracene; +0.96 V vs Fc/Fc$^+$ for 9-bromoanthracene; +0.67 and −0.81 V vs Fc/Fc$^+$ for 9-(*p*-tolylethynyl)anthracene; and +0.36, +0.88, and −0.95 V vs Fc/Fc$^+$ for 9-(*N*,*N*-diphenyl-4-anilino)anthracene], suggesting that the conjoined anthryl units remain orthogonal in the first-charged redox states as well. Previous experimental and theoretical studies on 9,9′-bianthryl showed that their structural rigidity, steric crowdedness, and conformation in the radical ion state resemble those of the precursors. The dihedral angles between the two π units in 9,9′-bianthryl$^{+\bullet}$ [30] and 9,9′-bianthryl$^{-\bullet}$ [31] are ca. 77 ± 3° and 80 ± 2°, respectively, in close agreement with that of neutral 9,9′-bianthryl (82 ± 2°).[6] Therefore, the conformational change during oxidation or reduction is of minor importance.[26] It is worth mentioning that all of the bianthryls in Chart 2 benefit from the steric crowding around the redox unit,

dx.doi.org/10.1021/jo401785c | J. Org. Chem. 2013, 78, 10383−10394

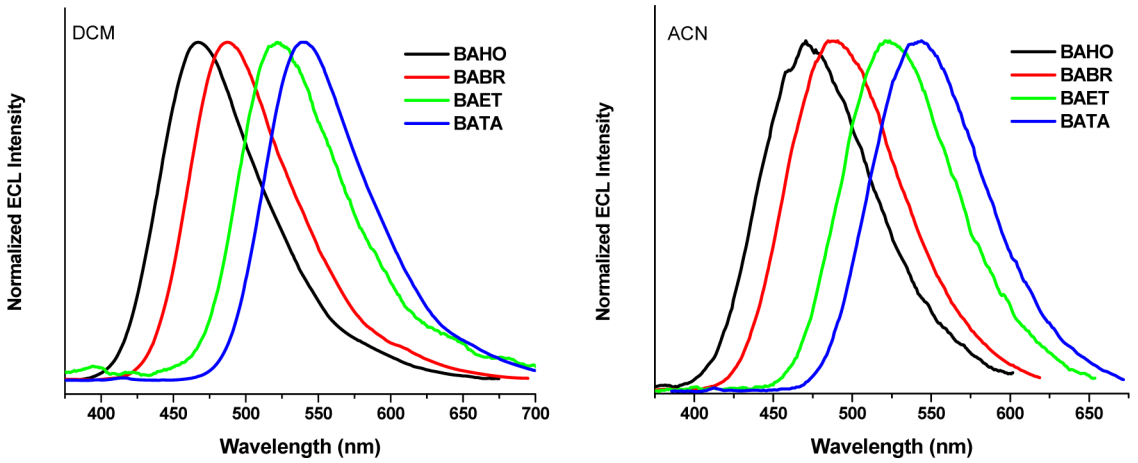

Figure 4. ECL spectra of **BAHO**, **BABR**, **BAET**, and **BATA** (5×10^{-4} M) in (left) DCM and (right) ACN in the presence of 0.1 M TPrA and 0.1 M $TBAPF_6$.

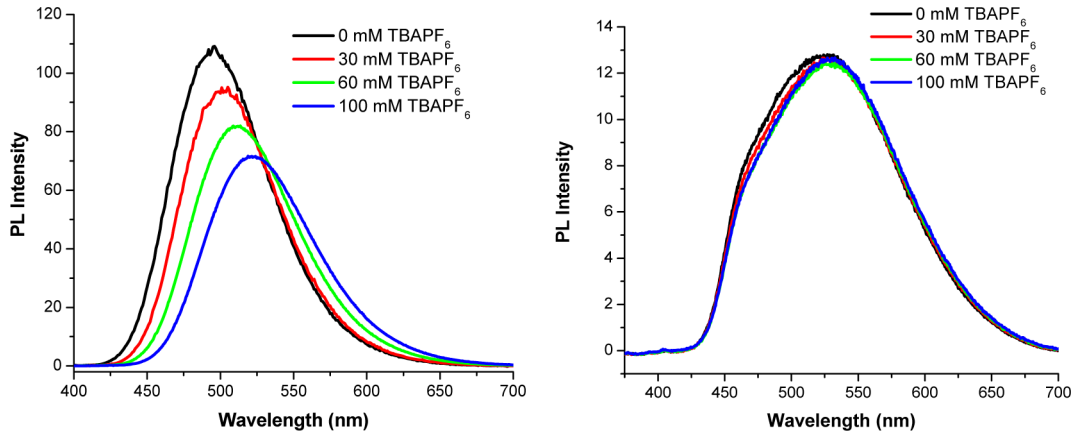

Figure 5. PL titrations of **BATA** with $TBAPF_6$ in (left) DCM and (right) ACN using excitation at 360 ± 5 nm. There are significant red shifts in λ_{max}^{PL} and losses in emission intensity with increasing $TBAPF_6$ concentration. The effect is more pronounced in DCM than in ACN.

as they show rather stable redox behavior leastwise for one-electron oxidation and reduction (except **BABR**). In contrast, polycyclic aromatic hydrocarbons often lack electrochemical stability under ambient conditions because of self-quenching and reactions with impurities even in purified solvent/electrolyte systems.[3]

Electrochemiluminescence. The ECL behavior of the bianthryls in Chart 2 was explored because their high ϕ_{PL} and appreciable redox stability are ideal prerequisites for high ECL activity.[1,2,32] ECL was recorded in an oxidative−reduction protocol employing tri-*n*-propylamine (TPrA) as a coreactant and $TBAPF_6$ as a supporting electrolyte in both DCM and ACN.[33] The ECL signal was produced by sweeping the electrode potential reversibly from +0.1 to +1.1 V vs Ag/Ag^+ at 0.1 V s^{-1} and by employing different concentrations of the luminophore [(1−7) × 10^{-4} M]. Satisfactory ECL spectra with a defined emission maximum were noticed starting at concentrations above 4×10^{-4} M, while no emission was observed in the absence of either the luminophore or the coreactant. The ECL data for all of the compounds are given in Figure 4 and Table 2.

All of the bianthryls were found to be ECL-active, affording intense signals in both DCM and ACN. Independent of the luminophore concentration and medium (i.e., DCM or ACN), the profiles were unstructured and the ECL wavelength maxima (λ_{max}^{ECL}) were closely similar, shifted just about ±2−3 nm. Comparing the ECL and PL spectra, we found close agreement in ACN only. In this event, the λ_{max}^{ECL} values for **BAHO**, **BABR**, **BAET**, and **BATA**, respectively, are 472, 487, 522, and 537 nm (Table 2) while the λ_{max}^{PL} values are 462, 483, 519, and 528 nm (Table 1) suggesting that the emission arises from the same excited state.[1] In contrast, in DCM the shape of the ECL band and λ_{max}^{ECL} do not coincide with those from PL. For example, the PL spectra are partially structured, whereas unstructured profiles are received in ECL (Figure 4). Also, the λ_{max}^{ECL} values in DCM (at 469, 486, 520, and 538 nm, respectively) are red-shifted by ca. 20−40 nm relative to λ_{max}^{PL} = 446, 457, 490, and 496 nm, respectively (Table 1). The inconsistency of the ECL and PL findings in DCM suggested to us to explore the effect of the supporting electrolyte on the PL, since the electrolyte might change the polarity of the medium (Figure 5).[19] Interestingly, with increasing amount of $TBAPF_6$, the PL shifted bathochromically, with a maximum shift of 25 ± 3 nm in DCM and <5 nm in ACN (Tables 1 and 2). The values of λ_{max}^{PL} in DCM containing $TBAPF_6$ (0.1 M) are 468, 482, 517, and 524 nm for **BAHO**, **BABR**, **BAET**, and **BATA**, respectively (Figure 5; also see the SI). These values are slightly smaller (<10 nm) than the λ_{max}^{ECL} in DCM (Figure 4), possibly as a result of a concentration effect, as is often observed in ECL studies.[1,2] In summary, the ECL emission of the bianthryls in Chart 2 in either DCM or ACN originates from the same excited state as in the PL in ACN (cf. Tables 1 and 2). Furthermore, the ECL signal is assigned solely to the CT state, with no emission arising from either the LE or excimer state.[32]

dx.doi.org/10.1021/jo401785c | J. Org. Chem. 2013, 78, 10383−10394

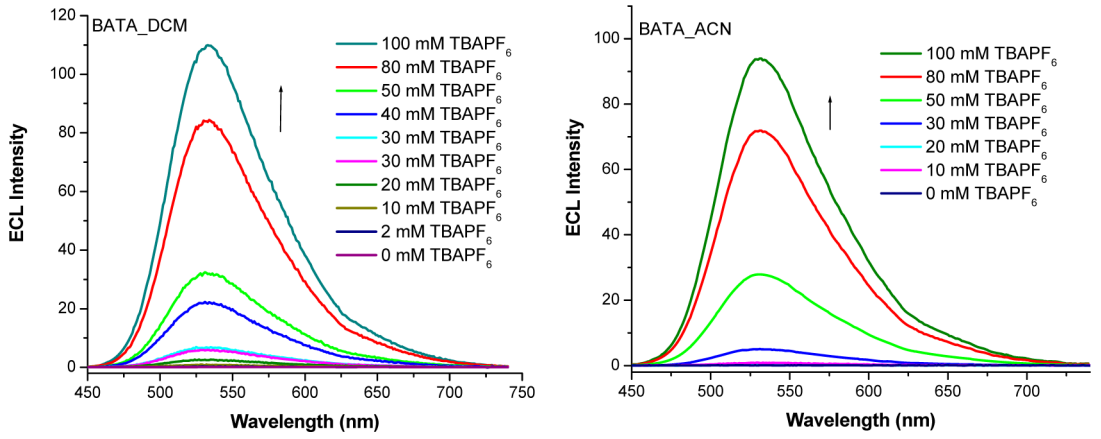

Figure 6. ECL spectra of **BATA** in (left) DCM and (right) ACN taken in the presence of various amounts of $TBAPF_6$.

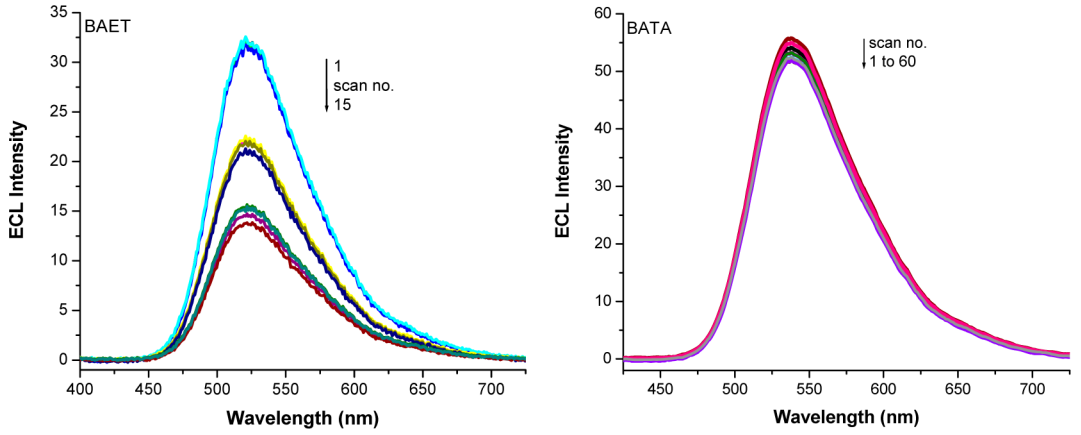

Figure 7. ECL of (left) **BAET** and (right) **BATA** recorded in DCM with repeated potential scans. The ECL intensity of **BAET** decreases with subsequent scans, whereas there is no significant change in ECL intensity of **BATA** even after ca. 60 cycles. A pale-yellow film was formed at the electrode surface with every 4−6 subsequent scans and had to be removed to maintain some emission in subsequent scans of **BAET**.

In order to check the ECL for high-energy emission (LE, Scheme 2) as seen in the PL spectra of the bianthryls in DCM, we explored ECL at diverse $TBAPF_6$ concentrations ranging from 10 to 100 mM.[34] ECL experiments were performed only for **BATA** because of its good redox stability.[35] As anticipated, at low concentrations of $TBAPF_6$ (10−30 mM) the number of radical ions formed is small, and thus, an insignificant ECL signal is seen (Figure 6).[1,2] Above 40 mM $TBAPF_6$, because of the increasing solution conductivity, ECL intensity emerges at $\lambda_{max}^{ECL} = 536 \pm 2$ nm but shows only an unstructured profile. Thus, the higher-energy band encountered in the PL of bianthryls (Chart 2 and Figure 2) is completely absent in the ECL spectra (Figure 6) because of the prevalence of the CT state over the LE state (Scheme 2).[32] An analogous situation has been detected in several bichromophoric donor−acceptor molecules that show solvatochromic emission in PL but unique CT emission in ECL.[36]

The ECL intensity was determined as a function of the substituents while keeping closely identical conditions for all of the experiments. While the ECL intensity follows the series **BATA** ≫ **BABR** > **BAHO** ≈ **BAET**, the PL intensity sequence is **BATA** > **BAET** > **BAHO** > **BABR** (Table 1). Perceptibly, **BATA** yields the highest emission intensity in both channels. For a better measure, the ECL intensities of bianthryls were quantified by relative ECL efficiency[37] (ϕ_{ECL}, given by the integrated light intensity under an emission curve) using DPA as a standard (Table 2). The value of ϕ_{ECL} for **BATA** is 3 times higher than that for **BAET**/**BAHO** and 2 times higher than that for **BABR**. Likewise, ϕ_{ECL} for **BABR** is 1.5 times higher than those for **BAET** and **BAHO** (Table 2). A quantitative comparison of ϕ_{PL} and ϕ_{ECL} does not show any overall relationship. For example, ϕ_{PL}(**BABR**) = 0.1 in DCM is about 7 times smaller than ϕ_{PL}(**BAET**) = 0.68, while ϕ_{ECL} for the former is twice as large as the latter, obviously because of the complexity of ECL generation.[2,37] The very high ECL intensity of **BATA** (Table 2) compared with those of other compounds is due to the good steric protection of the reactive 10,10′-positions of the bianthryl residue and efficient ICT from the energetically higher lying LE state to the CT state (Scheme 2).[24,36] Likewise, the ECL intensity of triarylamine-decorated spirobifluorenes was found to be higher than that of the parent spirobifluorene because the radical cation stability was improved significantly by triarylamine substituents.[1,2a,4e,h]

The ECL stabilities of the bianthryls in Chart 2 over multiple scans were determined by pulsing the electrodes reversibly with the same bianthryl solution.[1,2] Compared with the parent **BAHO**, the λ_{max}^{ECL} values and emission intensities of **BABR** and **BATA** remained steady, even after 60 repeated cycles. In contrast, the signal intensities of **BAET** and **BAHO** decreased to 50% within 10 subsequent scans (Figure 7) and completely disappeared after 5−10 additional scans (vide infra) despite a reversible first oxidation wave in the CV (Figure 3). Thus, the

dx.doi.org/10.1021/jo401785c | J. Org. Chem. 2013, 78, 10383−10394

ECL signal stability over multiple cycles at a fixed scan rate decreases in the following order: **BATA** ≈ **BABR** > **BAHO** > **BAET** in both DCM and ACN.

Within the bianthryl series in Chart 2, **BAET** underwent the most pronounced degradation with increasing number of scans, exhibiting a thin pale-yellow film on the electrode surface that could be removed by polishing prior to reexamining the ECL. Nevertheless, the intensity was not restored over multiple cycles (Figure 7), suggesting instability of the radical ion of **BAET** to yield byproducts.[1,2,27a]

Both **BABR** and **BATA** showed remarkable ECL stability over many scans (Figure 7; also see the SI), suggesting that their substituents effectively prevent electrochemical decomposition of the bianthryl unit.[9] The triarylamine motif has been known to enhance the thermal and electrochemical stabilities of several chromophores.[3,5] For instance, triarylamine derivatives have been employed as hole-transporting materials in light-emitting devices.[11c,38] Likewise, the bromo substituents in **BABR** protect the emitting bianthryl unit against decomposition via steric protection, as is known for tris(4-bromophenyl)aminium hexachloroantimonate in comparison with triphenylaminium salts.[39] Thus, the bromo- and triarylamine-substituted bianthryls **BABR** and **BATA** both furnish novel and redox-stable ECL emissive materials that show luminescence from the CT state. In contrast, LE state emission generally has been noticed from the analogous bulky and rigid ECL emitters shown in Chart 1.[4] The gentle accessibility, nice solubility in various organic solvents, and robust redox and ECL qualities of the 9,9′-bianthryl scaffold (Chart 2) pave the way for the development of a myriad of awkwardly shaped materials with desirable properties.

CONCLUSIONS

9,9′-Bianthryl (**BAHO**) and its 10,10′-substituted derivatives **BABR**, **BAET**, and **BATA** have been synthesized in good yields from readily available precursors, and their photophysical, electrochemical, and ECL properties have been investigated. The mutual steric hindrance implemented into the bianthryl unit upgrades its functional utility relative to anthracene as its half-component. Highly stable ECL requires additional protection of the reactive centers of bianthryls at C10 and C10′ using suitable functional groups. The most stable ECL emitters as tested in multiple consecutive potential scans were the bromo- and triarylamine-functionalized bianthryls **BABR** and **BATA**, respectively, indicating that 10,10′-functionalized 9,9′-bianthryls are promising stable organic ECL emitters.

In summary, the present investigation underlines the value of the bianthryl scaffold as a readily tunable and intense ECL emitter with the prospect of long durability. In particular, the influence of peripheral groups is large, much more dominant than in inorganic materials. We therefore believe that this family of organic ECL emitters may find use as emissive tags and organic functional materials, including organic light-emitting diodes, organic field-effect transistors, organic photovoltaics, and organic lasers as well as in memory cells.

EXPERIMENTAL SECTION

General Aspects. Dry THF and toluene were distilled over potassium and sodium, whereas, CCl_4 and Et_3N were distilled over CaH_2 and KOH, respectively, prior to use. All of the reactions (except bromination) and distillations were performed in oven-dried glassware under a nitrogen gas atmosphere. Reactions were monitored by analytical thin-layer chromatography (TLC) on silica gel. Column chromatography was conducted with silica gel (60−120 mesh). All commercial chemicals were used as received. Measurements were carried out under ambient conditions unless stated otherwise. ^{1}H, ^{13}C, and COSY NMR spectra were recorded in deuterated solvents. Chemical shifts (δ) are reported in parts per million and are referenced to the residual protiated solvent.

Solutions (1×10^{-5} M) in 10 mm quartz cuvettes were used to record the absorption spectra of all samples. Likewise, PL spectra and quantum yields (ϕ_{PL}) were measured in 10 mm quartz cuvettes at concentrations of $(1-10) \times 10^{-6}$ M using $\lambda_{exc} = 360 \pm 5$ nm and excitation and emission slits set to either 1.5 or 2.5 nm. The ϕ_{PL} values were determined using DPA as a standard ($\phi_{PL} = 0.9 \pm 0.02$ in cyclohexane[25]). The following equation was used for the calculation of ϕ_{PL} for all samples:

$$\phi_u = \phi_s \frac{I_u}{I_s}\frac{A_s}{A_u}\left(\frac{\eta_u}{\eta_s}\right)^2$$

where the subscripts "s" and "u" refer to standard and unknown samples, A_u and A_s are the absorbances of the sample and the standard at the excitation wavelength, I_u and I_s are the integrated emission intensities (i.e., areas under the emission curves) of the sample and the standard, and η_u and η_s are the refractive indexes of the corresponding solvents.

CVs were obtained in a Pyrex cell containing a standard three-electrode setup (i.e., a 1 mm platinum disk working electrode, a platinum wire counter electrode, and a silver wire as a pseudoreference electrode) connected to a potentiostat. The working electrode in each case was polished on a felt pad with an alumina slurry (50−100 nm) and then rinsed with water followed by acetone and subsequently dried with air. $TBAPF_6$ and Fc were used as the supporting electrolyte and internal standard, respectively. Potentials were measured at a scan rate of 50 mV s^{-1} for oxidation in DCM and 100 mV s^{-1} for reduction in ACN. Solutions for both electrochemical oxidation and reduction experiments contained the sample/compound of interest at 5×10^{-4} M, the supporting electrolyte (0.1 M), and dry solvents. Prior to each experiment, solutions were deaerated by bubbling N_2 gas through them.

ECL measurements were recorded at room temperature in a Pyrex cell with a flat Pyrex window at the bottom for ECL monitoring. An analogous electrode setup as in the CV experiment was used. To generate ECL, the potential was swept across the first oxidation potential (+0.1 to +1.1 to +0.1 V with respect to a silver wire as a quasi-reference electrode) at 0.1 V s^{-1}. The resulting emission spectra were recorded with a CCD camera cooled to -50 ± 5 °C. Solutions for ECL contained 5×10^{-4} M sample, 0.1 M $TBAPF_6$, and 0.05−0.1 M TPrA as a coreactant in either DCM or ACN.

The ECL emission was quantified by determination of the "relative ECL efficiency (ϕ_{ECL})"[37] using the following equation:

$$\phi_{ECL} = \phi^{\circ}_{ECL}\frac{I}{Q}\frac{Q^{\circ}}{I^{\circ}}$$

where ϕ_{ECL} and ϕ°_{ECL} are the ECL efficiencies of the target and standard samples, I and I° are integrated ECL intensities (areas under the curve) of the target and standard systems, and Q and Q° are the charges passed for the target and standard, respectively. We used DPA as a standard with the assumption that its quantum efficiency is equal to 1. In order to maintain the equal number of charges for the target/coreactant and standard/coreactant systems during ECL sweeping, we performed the experiments under exactly similar conditions,[2a,37] meaning we employed same electrodes, solvent, electrolyte, coreactant and concentrations throughout the estimation of ϕ_{ECL}.

Preparation of 4-*N*,*N*-Diphenylaminophenylboronic Acid. To a solution of 4-bromo-*N*,*N*-diphenylaniline (2.0 g, 6.2 mmol) in THF (60 mL) kept at −50 to −60 °C (with the low temperature maintained by using an acetone/liquid nitrogen bath) was added *n*BuLi (6.5 mmol) dropwise over 30 min. The resultant green-colored solution was stirred for 30 min at the same temperature, after which trimethyl borate (1.1 mL, 9.3 mmol) was added slowly. The reaction mixture was brought to room temperature over a period of 2 h, and then aqueous NH_4Cl (5 mL) was added. The volatiles were removed, and the organic material was extracted with ethyl acetate. The combined extracts were dried over Na_2SO_4 and evaporated. The pure product was obtained after filtration

dx.doi.org/10.1021/jo401785c | J. Org. Chem. 2013, 78, 10383−10394

over a short pad of silica gel using 40% ethyl acetate in hexane followed by recrystallization from ethyl acetate and hexane, which furnished 4-*N*,*N*-diphenylaminophenylboronic acid as light-yellow solid (1.1 g, 62%). Mp 220−224 °C (lit 218 °C[40]); R_f 0.52 in 50% ethyl acetate in hexane; ^{1}H NMR (400 MHz, CD_2Cl_2) δ 7.04−7.15 (m, 8H, 6/7/9-H), 7.29 (t, J = 8.4 Hz, 4H, 8-H), 8.01 (d, J = 8.4 Hz, 2H, 5-H); ^{13}C NMR (100 MHz, CD_2Cl_2) δ 120.7, 124.0, 125.6, 129.5 (×2), 136.7, 147.2, 151.8.

Preparation of 9,9′-Bianthryl (BAHO). BAHO was prepared in two steps. First, 9-anthrone (10 g, 52 mmol) was added to a suspension of Zn powder (17.0 g, 258 mmol) and $ZnCl_2$ (14.0 g, 103 mmol) in aqueous THF (70:30 v/v THF/H_2O, 100 mL). The resultant slurry was stirred at room temperature until all of the Zn particles had disappeared (duration ca. 36 h). Thereafter the volatiles were removed and the organic matter extracted with DCM. The combined DCM layers were dried over Na_2SO_4. After evaporation of the solvent and drying in vacuo, the obtained pale-yellow solid (8.3 g) was used without further purification. An 8.0 g sample was added to a solution of a catalytic amount of *p*-toluenesulfonic acid (30 mg) in toluene (120 mL). The solution was refluxed for 2 h, during which the mixture changed from a cloudy-white to clear solution with increasing blue luminescent emission. Subsequently, toluene was removed, and the solid residue was purified by silica gel column chromatography using 2−4% CH_2Cl_2 in hexane, yielding 9,9′-bianthryl as a pale-yellow crystalline solid (6.6 g, 91%). Mp 311−315 °C (lit 314 °C[6b,g,41]); R_f 0.47 in hexane; ^{1}H NMR (400 MHz, CD_2Cl_2) δ 7.03 (ddd, J = 8.8, 1.2. 0.8 Hz, 4H, 1/1′/8/8′-H), 7.13 (ddd, J = 8.8, 6.6, 1.2 Hz, 4H, 2/2′/7/7′-H), 7.45 (ddd, J = 8.4, 6.6, 1.0 Hz, 4H, 3/3′/6/6′-H), 8.16 (ddd, J = 8.4, 0.8, 0.4 Hz, 4H, 4/4′/5/5′-H), 8.71 (s, 2H, 10/10′-H); ^{13}C NMR (100 MHz, CD_2Cl_2) δ 125.4, 125.9, 126.6, 127.4, 128.7, 131.6, 131.7, 133.0.

Preparation of 10,10′-Dibromo-9,9′-bianthryl (BABR). A solution of bromine (0.900 mL, 0.017 mol) in CCl_4 (60 mL) was added dropwise over a period of 2 h to a solution of 9,9′-bianthryl (3.0 g, 8.5 mmol) in CCl_4 (150 mL) at 0 °C. After the addition was complete, the ice bath was removed, and the contents were stirred at room temperature for additional 2 h. Subsequently, the mixture was diluted with CH_2Cl_2 (100 mL), washed well with 2 N NaOH, and dried over anhydrous Na_2SO_4. The solid obtained after evaporation was purified by silica gel column chromatography using 2−4% CH_2Cl_2 in hexane, yielding 10,10′-dibromo-9,9′-bianthryl as a lemon-yellow solid (3.7 g, 86%). Mp >320 °C (lit 357−359 °C[16]); R_f 0.51 in hexane; ^{1}H NMR (400 MHz, CD_2Cl_2) δ 7.05 (ddd, J = 8.8, 0.8, 0.4 Hz, 4H, 1/1′/8/8′-H), 7.18 (ddd, J = 8.8, 6.4, 1.2 Hz, 4H, 2/2′/7/7′-H), 7.58 (ddd, J = 9.2, 6.8, 1.2 Hz, 4H, 3/3′/6/6′-H), 8.69 (ddd, J = 9.2, 0.8, 0.4 Hz, 4H, 4/4′/5/5′-H); ^{13}C NMR (100 MHz, CD_2Cl_2) δ 123.9, 126.4, 127.1, 127.4, 128.1, 130.6, 132.3, 133.3.

Preparation of 10,10′-Bis(*N*,*N*-diphenyl-4-anilino)-9,9′-bianthryl (BATA). 10,10′-Dibromo-9,9′-bianthryl (800 mg, 0.200 mmol), 4-*N*,*N*-diphenylaminophenylboronic acid (1.0 g, 3.5 mmol), and [$Pd(PPh_3)_4$] (0.18 g, 10 mol %) were introduced into a pressure tube under N_2. The N_2 was purged (10−15 min), and then toluene (30 mL) and aqueous $NaHCO_3$ (7 mL) were added to this mixture. Afterward, the tube was sealed, and the reaction mixture was heated at 90−100 °C for 12 h and then cooled to room temperature. The contents were extracted with CH_2Cl_2 and dried over Na_2SO_4. The material received after evaporation of the solvent was purified by column chromatography (silica gel) using 5−10% CH_2Cl_2 in hexane, yielding 10,10′-bis(*N*,*N*-diphenyl-4-anilino)-9,9′-bianthryl as a crystalline yellow solid (1.0 g, 74%). Mp 306−310 °C; R_f 0.22 in 20% DCM in hexane; IR (KBr) 3074, 3064, 3049, 2955, 2925, 2855, 1948, 1942, 1936, 1586, 1519, 1465, 1454, 1403, 1378, 1330, 1318, 1268, 1151, 1075, 1011, 954, 893, 885, 859, 851, 838, 784, 760 cm^{-1}; ^{1}H NMR (400 MHz, CD_2Cl_2) δ 7.07−7.20 (m, 12H, 1/1′/2/2′/7/7′/8/8′/12/12′-H), 7.27−7.29 (m, 8H, 16/16′-H), 7.33−7.39 (m, 16H, 3/3′/6/6′/17/17′/18/18′-H), 7.48 (ddd, J = 8.8, 2.2, 0.4 Hz, 4H, 4/4′/5/5′-H), 7.96 (d, J = 8.8 Hz, 4H, 12/12′-H); ^{13}C NMR (100 MHz, CD_2Cl_2) δ 123.5, 123.7, 125.0, 125.5, 125.9, 127.2, 127.8, 129.8, 130.7, 131.8, 132.6, 133.0, 133.6, 138.3, 147.7, 148.2. Anal. calcd for $C_{64}H_{44}N_2$: C, 91.40; H, 5.27; N, 3.33. Found: C, 91.38; H, 5.28; N, 3.37.

Preparation of 10,10′-Bis(*p*-tolylethynyl)-9,9′-bianthryl (BAET). An oven-dried pressure tube was cooled under N_2 and then charged with 10,10′-dibromo-9,9′-bianthryl (1.0 g, 2.0 mmol), *p*-tolylethyne (0.70 mL, 5.0 mmol), [$Pd(PPh_3)_4$] (0.23 g, 10 mol %), CuI (12.0 mg, 3 mol %), Et_3N (10 mL), and THF (20 mL). Subsequently, the tube was sealed, and the mixture was heated at 70−80 °C for 36 h. After the reaction mixture had been cooled, the contents were extracted with CH_2Cl_2 and dried over Na_2SO_4. The brown residue received after evaporation of the solvents was purified by column chromatography over silica gel using 5−10% CH_2Cl_2 in hexane to furnish 10,10′-bis(*p*-tolylethynyl)-9,9′-bianthryl as a yellowish-green powder (1.1 g, 89%). Mp >320 °C; R_f 0.62 in 20% DCM in hexane; IR (KBr) 3881, 3247, 3046, 3006, 2979, 2922, 2853, 2728, 1909, 1658, 1616, 1440, 1315, 1211, 1185, 1037, 1012, 885, 857, 835, 783 cm^{-1}; ^{1}H NMR (400 MHz, CD_2Cl_2) δ 2.45 (s, 6H, 15/15′-H), 7.10 (ddd, J = 8.8, 0.8, 0.4 Hz, 4H, 1/1′/8/8′-H), 7.20 (ddd, J = 8.8, 6.4, 1.2 Hz, 4H, 2/2′/7/7′-H), 7.33 (d, J = 8.4 Hz, 4H, 13/13′-H) 7.67 (ddd, J = 8.8, 6.4, 1.2 Hz, 3/3′/6/6′-H), 7.75 (d, J = 8.4 Hz, 4H, 12/12′-H), 8.83 (ddd, J = 8.8, 0.8, 0.4 Hz, 4H, 4/4′/5/5′-H); ^{13}C NMR (100 MHz, CD_2Cl_2) δ 21.4, 85.7, 88.6, 120.4, 120.6, 126.4, 126.7, 127.1, 127.2, 129.5, 131.3, 131.6, 132.4, 134.1, 139.3. Anal. calcd for $C_{46}H_{30}$: C, 94.81; H, 5.19. Found: C, 94.82; H, 5.19.

■ ASSOCIATED CONTENT

Supporting Information

Additional UV−vis, PL, excitation, CV, and ECL figures and NMR spectra for intermediates and final compounds. This material is available free of charge via the Internet at http://pubs.acs.org.

■ AUTHOR INFORMATION

Corresponding Authors

*E-mail: natarajan@chemie.uni-siegen.de.
*E-mail: schmittel@chemie.uni-siegen.de.

Notes

The authors declare no competing financial interest.

■ ACKNOWLEDGMENTS

We thank the Alexander von Humboldt Foundation for a postdoctoral research fellowship to P.N. In addition, we are indebted to the DFG under Schm 647/17-1 and Dr. S. Samanta for help with the NMR measurements.

■ REFERENCES

(1) *Electrogenerated Chemiluminescence*; Bard, A. J., Ed.; Marcel Dekker: New York, 2004.

(2) (a) *Materials Science and Technology*; Hutagalung, S. D., Ed.; InTech: Rijeka, Croatia, 2012. (b) Richter, M. M. *Chem. Rev.* **2004**, *104*, 3003. (c) Pascal, R. A., Jr. *Chem. Rev.* **2006**, *106*, 4809. (d) Saragi, T. P. I.; Spehr, T.; Siebert, A.; Fuhrmann-Lieker, T.; Salbeck, J. *Chem. Rev.* **2007**, *107*, 1011. (e) Miao, W. *Chem. Rev.* **2008**, *108*, 2506. (f) Kanibolotsky, A. L.; Perepichka, I. F.; Skabara, P. J. *Chem. Soc. Rev.* **2010**, *39*, 2695. (g) Hu, L.; Xu, G. *Chem. Soc. Rev.* **2010**, *39*, 3275. (h) Figueira-Duarte, T. M.; Müllen, K. *Chem. Rev.* **2011**, *111*, 7260. (i) Daimon, T.; Nihei, E. *J. Mater. Chem. C* **2013**, *1*, 2826.

(3) (a) Löb, W. *Electrochemistry of Organic Compounds*; Wiley: New York, 1906. (b) Popp, F. D.; Schultz, H. P. *Chem. Rev.* **1962**, *62*, 19. (c) Evans, D. S. *Chem. Rev.* **1990**, *90*, 739. (d) Heinze, J.; Frontana-Uribe, B. A.; Ludwigs, S. *Chem. Rev.* **2010**, *110*, 4724. (e) Sur, U. K. *Recent Trends in Electrochemical Science and Technology*; InTech: Rijeka, Croatia, 2012. (f) *Electrochemistry*; Khalid, M. A. A., Ed.; InTech: Rijeka, Croatia, 2013.

(4) (a) Rashidnadimi, S.; Hung, T. H.; Wong, K.-T.; Bard, A. J. *J. Am. Chem. Soc.* **2008**, *130*, 634. (b) Sartin, M. M.; Shu, C.; Bard, A. J. *J. Am. Chem. Soc.* **2008**, *130*, 5354. (c) Omer, K. M.; Ku, S.-Y.; Wong, K.-T.; Bard, A. J. *Angew. Chem., Int. Ed.* **2009**, *48*, 9300. (d) Omer, K. M.; Ku,

S.-Y.; Wong, K.-T.; Bard, A. J. *J. Am. Chem. Soc.* **2009**, *131*, 10733. (e) Omer, K. M.; Ku, S.-Y.; Cheng, J.-Z.; Chou, S.-H.; Wong, K.-T.; Bard, A. J. *J. Am. Chem. Soc.* **2011**, *133*, 5492. (f) Suk, J.; Wu, Z.; Wang, L.; Bard, A. J. *J. Am. Chem. Soc.* **2011**, *133*, 14675. (g) Suk, J.; Natarajan, P.; Moorthy, J. N.; Bard, A. J. *J. Am. Chem. Soc.* **2012**, *134*, 3451. (h) Polo, F.; Rizzo, F.; Veiga-Gutierrez, M.; Cola, L. D.; Quici, S. *J. Am. Chem. Soc.* **2012**, *134*, 15402.

(5) (a) Benmansour, H.; Shioya, T.; Sato, Y.; Bazan, G. C. *Adv. Funct. Mater.* **2003**, *13*, 883. (b) Wu, J.; Baumgarten, M.; Debije, M. G.; Warman, J. M.; Müllen, K. *Angew. Chem., Int. Ed.* **2004**, *43*, 5331. (c) Forrest, S. R.; Thompson, M. E. *Chem. Rev.* **2007**, *107*, 923. (d) Moorthy, J. N.; Venkatakrishnan, P.; Natarajan, P.; Huang, D.-F.; Chow, T. J. *J. Am. Chem. Soc.* **2008**, *130*, 17320. (e) Heremans, P.; Cheyns, D.; Rand, B. P. *Acc. Chem. Res.* **2009**, *42*, 1740. (f) *Materials Science—Advanced Topics*; Mastai, Y., Ed.; InTech: Rijeka, Croatia, 2013. (g) Pinaud, F.; Russo, L.; Pinet, S.; Gosse, I.; Ravaine, V.; Sojic, N. *J. Am. Chem. Soc.* **2013**, *135*, 5517.

(6) (a) Toda, F.; Tanaka, K.; Fujiwara, T. *Angew. Chem., Int. Ed. Engl.* **1990**, *29*, 662. (b) Tanaka, K.; Kishigami, S.; Toda, F. *J. Org. Chem.* **1990**, *55*, 2981. (c) Becker, H.-D.; Langer, V.; Sieler, J.; Becker, H. C. *J. Org. Chem.* **1992**, *57*, 1883. (d) Grozema, F. C.; Swart, M.; Zijlstra, R. W. J.; Piet, J. J.; Siebbeles, L. D. A.; van Duijnen, P. T. *J. Am. Chem. Soc.* **2005**, *127*, 11019. (e) Jou, J.-H.; Wang, C.-P.; Wu, M.-H.; Chiang, P.-H.; Lin, H.-W.; Li, H.-C.; Liu, R.-S. *Org. Electron.* **2007**, *8*, 29. (f) Kyzioł, J. B.; Zaleski, J. *Acta Crystallogr.* **2007**, *E63*, o1235. (g) Toyota, S.; Okamoto, Y.; Ishikawa, T.; Iwanaga, T.; Yamada, M. *Bull. Chem. Soc. Jpn.* **2009**, *82*, 182.

(7) (a) Schwab, P. F. H.; Levin, M. D.; Michl, J. *Chem. Rev.* **1999**, *99*, 1863. (b) Slayden, S. W.; Liebman, J. F. *Chem. Rev.* **2001**, *101*, 1541.

(8) Aubry, J.-M.; Pierlot, C.; Rigaudy, J.; Schmidt, R. *Acc. Chem. Res.* **2003**, *36*, 668.

(9) (a) Heinze, J. *Angew. Chem., Int. Ed. Engl.* **1981**, *20*, 202. (b) Dietrich, M.; Mortensen, J.; Heinze, J. *Angew. Chem., Int. Ed. Engl.* **1985**, *24*, 508. (c) Grampp, G.; Kapturkiewicz, A.; Salbeck, J. *Chem. Phys.* **1994**, *187*, 391.

(10) (a) Sioda, R. E. *J. Phys. Chem.* **1968**, *72*, 2322. (b) Hammerich, O.; Parker, V. D. *J. Am. Chem. Soc.* **1974**, *96*, 4289. (c) Fudickar, W.; Linker, T. *Chem.—Eur. J.* **2006**, *12*, 9276. (d) Matsubara, Y.; Kimura, A.; Yamaguchi, Y.; Yoshida, Z. *Org. Lett.* **2008**, *10*, 5541. (e) Zehm, D.; Fudickar, W.; Hans, M.; Schilde, U.; Kelling, A.; Linker, T. *Chem.—Eur. J.* **2008**, *14*, 11429. (f) Xia, Z.-Y.; Su, J.-H.; Wong, W.-Y.; Wang, L.; Cheah, K.-W.; Tian, H.; Chen, C. H. *J. Mater. Chem.* **2010**, *20*, 8382.

(11) (a) Cui, W.; Wu, Y.; Tian, H.; Geng, Y.; Wang, F. *Chem. Commun.* **2008**, 1017. (b) Szaciłowski, K. *Chem. Rev.* **2008**, *108*, 3481. (c) *Advances in Nanocomposites—Synthesis, Characterization and Industrial Applications*; Reddy, B. S. R., Ed.; InTech: Rijeka, Croatia, 2011.

(12) (a) Schmittel, M.; Lin, H.-W.; Thiel, E.; Meixner, A. J.; Ammon, H. *Dalton Trans.* **2006**, 4020. (b) Schmittel, M.; Lin, H.-W. *Angew. Chem., Int. Ed.* **2007**, *46*, 893. (c) Schmittel, M.; Lin, H.-W. *Inorg. Chem.* **2007**, *46*, 9139. (d) Schmittel, M.; Lin, H.-W. *J. Mater. Chem.* **2008**, *18*, 333. (e) Lin, H.-W.; Cinar, M. E.; Schmittel, M. *Dalton Trans.* **2010**, *39*, 5130. (f) Qinghai, S.; Bats, J. W.; Schmittel, M. *Inorg. Chem.* **2011**, *50*, 10531. (g) Schmittel, M.; Qinghai, S. *Chem. Commun.* **2012**, *48*, 2707. (h) Khatua, S.; Samanta, D.; Bats, J. W.; Schmittel, M. *Inorg. Chem.* **2012**, *51*, 7075. (i) Qinghai, S.; Birlenbach, L.; Schmittel, M. *Inorg. Chem.* **2012**, *51*, 13123. (j) Natarajan, P.; Schmittel, M. *Inorg. Chem.* **2013**, *52*, 8579.

(13) Natarajan, P.; Schmittel, M. *J. Org. Chem.* **2012**, *77*, 8669.

(14) (a) Kaug, T. J.; Jarzeba, W.; Barbara, P. F. *Chem. Phys.* **1990**, *149*, 81. (b) Bhattacharyya, K.; Chowdhury, M. *Chem. Rev.* **1993**, *93*, 507. (c) Laguitton-Pasquier, H.; Pansu, R.; Chauvet, J.-P.; Collet, A.; Faure, J.; Lapouyade, R. *Chem. Phys.* **1996**, *212*, 437. (d) Józefowicz, M.; Fita, P.; Kasprzycki, P.; Heldt, J. R. *J. Phys. Chem. A* **2013**, *117*, 4136.

(15) Although, the photophysical properties of the parent 9,9′-bianthryl have already been reported (cf. ref 14), we examined it along with the other derivatives **BABR**, **BAET**, and **BATA** using identical experimental conditions for ready comparison.

(16) Müller, U.; Baumgarten, M. *J. Am. Chem. Soc.* **1995**, *117*, 5840.

(17) (a) Zander, M.; Rettig, W. *Chem. Phys. Lett.* **1984**, *110*, 602. (b) Rettig, W.; Majenz, W.; Lapouyade, R.; Vogel, M. *J. Photochem. Photobiol. A: Chem.* **1992**, *65*, 95. (c) Grabowski, Z. R.; Rotkiewicz, K. *Chem. Rev.* **2003**, *103*, 3899.

(18) (a) Smith, M. J.; Krogh-Jespersen, K.; Levy, R. M. *Chem. Phys.* **1993**, *171*, 97. (b) Boyer, G.; Claramunt, R. M.; Elguero, J.; Fathalla, M.; Foces-Foces, C.; Jaime, C.; Llamas-Saiz, A. L. *J. Chem. Soc., Perkin Trans. 2* **1993**, 757.

(19) Lakowicz, J. R. *Principles of Fluorescence Spectroscopy*, 3rd ed.; Springer: New York, 2010.

(20) Hanson, K.; Patel, N.; Whited, M. T.; Djurovich, P. I.; Thompson, M. E. *Org. Lett.* **2011**, *13*, 1598.

(21) (a) Piet, J. J.; Schuddeboom, W.; Wegewijs, B. R.; Grozema, F. C.; Warman, J. M. *J. Am. Chem. Soc.* **2001**, *123*, 5337. (b) Asami, N.; Takaya, T.; Yabumoto, S.; Shigeto, S.; Hamaguchi, H.; Iwata, K. *J. Phys. Chem. A* **2010**, *114*, 6351. (c) Li, X.; Liang, M.; Chakraborty, A.; Kondo, M.; Maroncelli, M. *J. Phys. Chem. B* **2011**, *115*, 6592. (d) Whited, M. T.; Patel, N. M.; Roberts, S. T.; Allen, K.; Djurovich, P. I.; Bradforth, S. E.; Thompson, M. E. *Chem. Commun.* **2012**, *48*, 284.

(22) (a) Nagasawa, Y.; Itoh, T.; Yasuda, M.; Ishibashi, Y.; Ito, S.; Miyasaka, H. *J. Phys. Chem. B* **2008**, *112*, 15758. (b) Khara, D. C.; Paul, A.; Santhosh, K.; Samanta, A. *J. Chem. Sci.* **2009**, *121*, 309.

(23) (a) Pu, L. *Chem. Rev.* **1998**, *98*, 2405. (b) Feringa, B. L.; van Delden, R. A.; Koumura, N.; Geertsema, E. M. *Chem. Rev.* **2000**, *100*, 1789. (c) Vezzu, D. A. K.; Deaton, J. C.; Shayeghi, M.; Li, Y.; Huo, S. *Org. Lett.* **2009**, *11*, 4310.

(24) (a) Elangovan, A.; Kao, K. M.; Yang, S.-W.; Chen, Y.-L.; Ho, T.-I.; Su, Y. O. *J. Org. Chem.* **2005**, *70*, 4460. (b) Ho, H.-I.; Elangovan, A.; Hsu, H.-Y.; Yang, S.-W. *J. Phys. Chem. B* **2005**, *109*, 8626.

(25) Hamal, S.; Hirayama, F. *J. Phys. Chem.* **1983**, *87*, 83.

(26) The experimental peak separation (78 mV) was larger than expected for ideal Nernstian behavior (59 mV). However, the internal standard Fc/Fc^+ showed the same trend as well. This effect can be attributed to the ohmic drop of the system, as similarly noticed previously for aprotic media (cf. ref 3).

(27) (a) Zweig, A.; Maurer, A. H.; Roberts, B. G. *J. Org. Chem.* **1967**, *32*, 1322. (b) McCreery, R. *Chem. Rev.* **2008**, *108*, 2646. (c) Poriel, C.; Rault-Berthelot, J.; Thirion, D. *J. Org. Chem.* **2013**, *78*, 886.

(28) *Developments in Electrochemistry*; Chun, J. H., Ed.; InTech: Rijeka, Croatia, 2012.

(29) (a) Jaworski, J. S.; Leszczynski, P.; Filipek, S. *J. Electroanal. Chem.* **1997**, *4−10*, 163. (b) Girina, G. P.; Feoktistov, L. G.; Alpatova, N. M. *Russ. J. Electrochem.* **2002**, *38*, 1357.

(30) Nadeem Khan, M.; Palivan, C.; Barbosa, F.; Amaudrut, J.; Gescheidt, G. *J. Chem. Soc., Perkin Trans. 2* **2001**, 1522.

(31) Bock, H.; Havlas, Z.; Hess, D.; Näther, C. *Angew. Chem., Int. Ed.* **1998**, *37*, 502.

(32) Kapturkiewicz, A. *J. Electroanal. Chem.* **1993**, *348*, 283.

(33) All commercially available ECL analytical instruments are based on coreactant technology. In this protocol, the ECL signal is generated by spanning the electrode potential in a single direction (cf. ref 1).

(34) (a) Keszthelyl, C. P.; Tokel-Takvoryan, N. E.; Tachikawa, H.; Bard, A. J. *Chem. Phys. Lett.* **1973**, *23*, 219. (b) Copeland, T. R.; Christie, J. H.; Skogerboe, R. K.; Osteryoung, R. A. *Anal. Chem.* **1973**, *45*, 995. (c) Zhivnov, V. A.; Nemkovich, N. A.; Rumyantsev, I. Y.; Tomin, V. I. *Zh. Prikl. Spektrosk.* **1977**, *27*, 446. (d) Ciszkowska, M.; Stojek, Z. *Anal. Chem.* **1992**, *64*, 2372.

(35) Although the ECL spectra are obtained by pulsing the electrodes slightly beyond (ca. 100 mV) the first redox potential of the luminophore, there will always be some redox disproportionation to generate the dication. Thus, if the second redox reaction is electrochemically reversible (as for **BABR**, **BAET**, and **BATA**), the stability of the ECL should be improved significantly.

(36) (a) Kapturkiewicz, A.; Herbich, J.; Nowacki, J. *Chem. Phys. Lett.* **1997**, *275*, 355. (b) Elangovan, A.; Lin, J.-H.; Yang, S.-W.; Hsu, H.-Y.; Ho, T.-I. *J. Org. Chem.* **2004**, *69*, 8086. (c) Yang, S.-W.; Elangovan, A.; Ho, T.-I. *Photochem. Photobiol. Sci.* **2005**, *4*, 327. (d) Jiang, X.; Yang, X.; Zhao, C.; Jin, K.; Sun, L. *J. Phys. Chem. C* **2007**, *111*, 9595. (e) Shen, M.;

Rodríguez-López, J.; Lee, Y.-T.; Chen, C.-T.; Fan, F.-R. F.; Bard, A. J. *J. Phys. Chem. C* **2010**, *114*, 9772.
(37) Pyati, R.; Richter, M. M. *Annu. Rep. Prog. Chem., Sect. C* **2007**, *103*, 12.
(38) (a) Moorthy, J. N.; Venkatakrishnan, P.; Huang, D.-F.; Chow, T.-J. *Chem. Commun.* **2008**, 2146. (b) *Organic Light Emitting Diode*; Mazzeo, M., Ed.; Sciyo: Rijeka, Croatia, 2010.
(39) (a) Breslin, D. T.; Fox, M. A. *J. Org. Chem.* **1994**, *59*, 7557. (b) Naredla, R. R.; Klumpp, D. A. *Chem. Rev.* **2013**, *113*, 6905.
(40) Wang, D.; Wang, J.; Fan, H.-L.; Huang, H.-F.; Chu, Z.-Z.; Zou, X. C. *Inorg. Chim. Acta* **2011**, *370*, 340.
(41) Berke, C. M.; Streitwieser, A., Jr. *J. Organomet. Chem.* **1980**, *197*, 123.